Journal of
Synchrotron Radiation

ISSN 0909-0495

Received 24 May 2013
Accepted 28 July 2013

X-ray dynamical diffraction Fraunhofer holography

Minas Balyan

Yerevan State University, Faculty of Physics, Department of Solid State Physics, Alex Manoogian 1, 0025 Yerevan, Armenia. E-mail: mbalyan@ysu.am

An X-ray dynamical diffraction Fraunhofer holographic scheme is proposed. Theoretically it is shown that the reconstruction of the object image by visible light is possible. The spatial and temporal coherence requirements of the incident X-ray beam are considered. As an example, the hologram recording as well as the reconstruction by visible light of an absolutely absorbing wire are discussed.

Keywords: X-ray dynamical diffraction; X-ray holography; X-ray microscopy; image processing.

1. Introduction

In an earlier work by Aristov & Ivanova (1979), X-ray holographic schemes were analyzed. It was indicated that X-ray holography schemes can be constructed on the basis of the methods of X-ray diffraction optics. Nowadays, various X-ray holographic schemes are proposed: holographic methods in X-ray crystallography (Szöke, 1998; Anduleit & Materlik, 2003; Hau-Riege *et al.*, 2004), X-ray atomic-resolution holography (Novikov *et al.*, 1998), X-ray fluorescence holography (Chukhovskii & Poliakov, 2004), X-ray holography for mosaic crystals (Korecki *et al.*, 2004), X-ray diffuse-scattering holography (Kopecký, 2004) and grating-based holography (Nygård *et al.*, 2010).

In the visible-light optics various holographic schemes are used: Fresnel holography methods of in-line (Gabor) and off-axis holographies, Fraunhofer holography, Fourier holography and interferometric holography (Caulfield, 1979; Hariharan, 2002). The corresponding analogues in the hard X-ray region nowadays are presented [in all the hard X-ray holographic methods the reconstruction can be performed using visible light or numerical (mathematical) methods of reconstruction]: X-ray interferometric holography (Egiazaryan & Bezirganyan, 1980; Egiazaryan, 1998; Egiazaryan *et al.*, 1998, and references therein), X-ray in-line holography (Snigirev *et al.*, 1995; Nugent *et al.*, 1996; Paganin, 2006, and references therein), X-ray Gabor and Fourier holography (Leitenberger & Snigirev, 2001; Watanabe *et al.*, 2003; Iwamoto & Yagi, 2011, and references therein). According to the method of X-ray interferometric holography, a three (Egiazaryan & Bezirganyan, 1980; Egiazaryan, 1998) or four block (Egiazaryan *et al.*, 1998) X-ray Laue case interferometer must be used. An object is placed in one of the arms of the interferometer. The beam passing along the other arm of the interferometer is the reference wave. The hologram is recorded in one of the beams emerging from the third or fourth block of the interferometer. The subsequent illumination of the hologram by the light reconstructs the image of the object. In Momose's technique (Momose, 1995) the image reconstruction is performed by Fourier-transform mathematical methods of reconstruction. Gabrielyan (1990) proposed a method of reconstruction of the visible image of an X-ray point source. According to this method the crystal-diffraction X-ray image of a point source, placed on the entrance surface of a plane-parallel perfect crystalline plate, must be used. Two branches of a dispersion surface must be taken into account. The intensity of the diffraction pattern in the diffracted field (Kato's spherical pendelosung fringes) is recorded on a photographic plate. By illuminating this photographic plate by a wave of visible light, one reconstructs the X-ray point-source visible image. In the works of Leitenberger & Snigirev (2001) and Watanabe *et al.* (2003), the necessary X-ray point reference source is obtained as a result of focusing by an X-ray zone plate. X-ray Fourier and Gabor holograms are recorded in a vacuum. The reconstruction can be performed by X-rays, by visible light or using numerical methods of reconstruction. In the work of Iwamoto & Yagi (2011), hard X-ray Fourier holography for imaging nanoscale objects is used. Nanoscale objects have low scattering amplitudes. To overcome this problem the authors used arrays of such objects each with its own reference. Balyan (2010) pointed out the possibility of an X-ray dynamical diffraction Fourier holographic scheme based on double-slit dynamical diffraction.

In general, holograms can be recorded in a medium using radiation with any wavelength and can be reconstructed in another medium using radiation with another wavelength.

The scheme presented in this paper (Fig. 1) can be regarded as an X-ray dynamical diffraction Fraunhofer holography method. The hologram is recorded using hard X-ray dynamical diffraction in a perfect plane-parallel crystalline plate. The subsequent reconstruction can be performed using visible-light illumination of the hologram or numerical

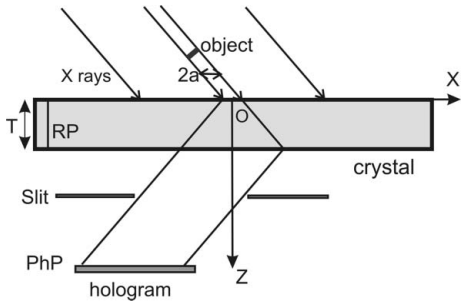

Figure 1
X-ray dynamical diffraction Fraunhofer hologram recording scheme. RP, reflecting planes. PhP, photographic plate. The axes of the coordinate system are shown.

(mathematical) methods of reconstruction. The theoretical background of the scheme is given and the proposed scheme is investigated theoretically.

2. X-ray dynamical diffraction Fraunhofer holography

For the holographic scheme of Fig. 1, the reference wave is a plane wave. The object is placed in the path of the incident plane wave. In the crystal, under the condition of two-wave dynamical Laue-case symmetrical diffraction, the reference plane wave and the object wave interfere and on the exit surface of the crystal an interference pattern is formed. By recording this interference pattern in the diffracted field, one obtains an X-ray hologram of the object. Illuminating the hologram by visible light or using numerical methods, the reconstruction of the object image is obtained.

2.1. X-ray Fraunhofer hologram recording

In the two-wave approximation the amplitude E_h of the diffracted wave of an X-ray beam in a crystal for the Laue symmetric case of diffraction can be presented as (Authier, 2001; Pinsker, 1982)

$$E_h = \int_{-\infty}^{+\infty} G(x-x', z)E^i(x', y)[1 - S(x', y)] \times \exp(ik\cos\theta_0\Delta\theta x')\,\mathrm{d}x', \quad (1)$$

where

$$G(x, z) = ik\chi_h C J_0\Big[\pi\cot\theta_0\big(z^2\tan^2\theta_0 - x^2\big)^{1/2}/\Lambda\Big] \times \exp[ik\chi_0 z/(2\cos\theta_0)]\,H(z\tan\theta_0 - |x|) /(4\sin\theta_0) \quad (2)$$

is the point-source function (the case of spherical-wave dynamical theory), $E^i(x', y)$ is the amplitude of the incidence wave, $S(x, y) = 1 - t(x, y)$ is the scattered amplitude of the object, $t(x, y)$ is the complex amplitude transmission coefficient of the object, λ is the wavelength of X-rays, $k = 2\pi/\lambda$ is the wavenumber, $\Lambda = \lambda\cos\theta_0/[C(\chi_h\chi_{\bar{h}})^{1/2}]$, C is the polarization factor ($C = 1$ for σ-polarization and $C = \cos2\theta_0$ for π-polarization), χ_0, χ_h, $\chi_{\bar{h}}$ are the crystal dielectric susceptibility Fourier components corresponding to the zero and **h** reflection, $\theta_0(\lambda)$ is the Bragg exact angle for the wavelength λ, $H(x)$ is the step function, $H(x) = 1$ if $x > 0$, $H(x) = 0$ if $x < 0$, and J_0 is the zero-order Bessel function. In Fig. 1 the coordinate system $Oxyz$, with Oy axes perpendicular to the diffraction plane, is shown. The diffraction vector **h** is anti-parallel to the Ox axis, θ is the angle between the direction of the incident beam and the reflecting planes, and $\Delta\theta = \theta - \theta_0(\lambda)$ is the deviation from the exact Bragg angle for given λ. $S(x, y)$ is defined in the range $x \in (-\infty, \infty)$, $y \in (-\infty, \infty)$ and is equal to 0 outside the object $x \notin (-a, a)$. The formula (1) can be presented as the sum of two terms. The first term in (1) is the wavefield amplitude $E_{h\,\mathrm{ref}}$ without any object (reference-wave amplitude) and the second term is the influence $E_{h\,\mathrm{obj}}$ of the object on the amplitude of the wavefield (object-wave amplitude). Thus,

$$E_h = E_{h\,\mathrm{ref}} + E_{h\,\mathrm{obj}}. \quad (3)$$

The intensity distribution over the exit surface of the crystal ($z = T$)

$$I_h = \big|E_h\big|^2 = \big|E_{h\,\mathrm{ref}}\big|^2 + E_{h\,\mathrm{ref}}E^*_{h\,\mathrm{obj}} + E^*_{h\,\mathrm{ref}}E_{h\,\mathrm{obj}} + \big|E_{h\,\mathrm{obj}}\big|^2. \quad (4)$$

Recording the intensity distribution (4) on a photographic plate gives the so-called hologram of the object.

2.2. X-ray reference wave

According to (1) and (3),

$$E_{h\,\mathrm{ref}} = iE^i_0\chi_h\exp\big[ik\chi_0 T/(2\cos\theta_0)\big]\exp(ik\cos\theta_0\Delta\theta x) \times \sin\Big[kT\big(\chi_h\chi_{\bar{h}} + \Delta\theta^2\sin^2 2\theta\big)^{1/2}/(2\cos\theta_0)\Big] /\big(\chi_h\chi_{\bar{h}} + \Delta\theta^2\sin^2 2\theta\big)^{1/2}, \quad (5)$$

where E^i_0 is the amplitude of the incident plane wave and T is the thickness of the crystal. Hereafter $E^i_0 = 1$ is taken.

Without loss of generality, for definiteness, the case of a centre-symmetrical crystal is considered. It is assumed that $\chi_0 = \chi_{0r} + i\chi_{0i}$, $\chi_h = \chi_{\bar{h}} = \chi_{hr} + i\chi_{hi}$, $\chi_{0r} < 0$, $\chi_{hr} = \chi_{\bar{h}r} < 0$, $\chi_{hi} = \chi_{\bar{h}i} > 0$, $\chi_{hi} \ll |\chi_{hr}|$, $\chi_{hi} \cong \chi_{0i} > 0$. In the case $\mu T \gg 1$, where $\mu = k\chi_{0i}$ is the normal linear absorption coefficient of the cryatal, only the weakly absorbing branch of the dispersion surface for σ-polarization can be taken into account. Thus, the amplitude of the reference wave can be written in the form

$$E_{h\,\mathrm{ref}} = -\exp\big[ik\chi_{0r}T/(2\cos\theta_0)\big]\exp\big[-\mu_d(p)T/(2\cos\theta_0)\big] \times \exp(ik\cos\theta_0\Delta\theta x)\exp\Big[i\pi T\big(1+p^2\big)^{1/2}/\Lambda_r\Big] /\Big[2\big(1+p^2\big)^{1/2}\Big], \quad (6)$$

where $\mu_d(p) = \mu[1 - (\chi_{hi}/\chi_{0i})/(1+p^2)^{1/2}]$ is the diffraction linear absorption coefficient for the weakly absorbing branch, $\Lambda_r = \mathrm{Re}\,\Lambda$ is the extinction length, $p = \Delta\theta\sin2\theta/|\chi_{hr}|$.

2.3. X-ray hologram of a point object

According to (1) and (3),

$$E_{h\,\mathrm{obj}} = -\int_{-\infty}^{\infty} G(x-x', T)S(x', y)\exp(ik\cos\theta_0\Delta\theta x')\,\mathrm{d}x'. \quad (7)$$

In the case of X-ray diffraction, the object can be regarded as a point object if $a \ll |\Lambda| \tan\theta_0/\pi$ (Slobodetskii & Chukhovskii, 1970). In this case, according to (7),

$$E_{h\,\mathrm{obj}} = -2a\tilde{S}(y)G(x, T), \tag{8}$$

where $\tilde{S}(y) = \int_{-\infty}^{\infty} S(x', y)\exp(ik\cos\theta_0\Delta\theta x')\,\mathrm{d}x'/(2a)$. In the case $k\cos\theta_0\Delta\theta a \ll \pi$,

$$\tilde{S}(y) = \int\limits_{-\infty}^{\infty} S(x', y)\,\mathrm{d}x'/(2a). \tag{9}$$

In the visible-light optics one of the simple and classical objects for holography is a completely absorbing wire, $S(x, y) = 1$ for $x \in (-a, a)$ and $S(x, y) = 0$ for $x \notin (-a, a)$ (Caulfield, 1979).

For the case $\pi T/|\Lambda| \gg 1$ the well known asymptotic behaviour of Bessel function $J_0(x) \simeq (2/\pi x)^{1/2}\cos(x - \pi/4)$ can be used. Using the identity $\cos(x - \pi/4) = \{\exp[i(x - \pi/4)] + \exp[-i(x - \pi/4)]\}/2$ as well as the approximation $(T^2\tan^2\theta_0 - x^2)^{1/2} \simeq T\tan\theta_0[1 - x^2/(2T^2\tan^2\theta_0)]$ and taking into account only the weakly absorbing mode of σ-polarization, the following expression from (8) can be obtained,

$$\begin{aligned} E_{h\,\mathrm{obj}} \simeq\ & 2a\left(\frac{2}{T\Lambda_r}\right)^{1/2}\exp(i\pi/4)\cot\theta_0\,\tilde{S}(y)\exp\left(\frac{i\pi T}{\Lambda_r}\right) \\ & \times \exp\left(\frac{ik\chi_{0r}T}{2\cos\theta_0}\right)\exp\left(-\frac{\mu_d(0)T}{2\cos\theta_0}\right) \\ & \times \exp\left(-\frac{i\pi x^2}{2T\Lambda_r\tan^2\theta_0}\right)\exp\left(-\frac{\pi x^2\eta}{2T\Lambda_r\tan^2\theta_0}\right) \\ & \times H(T\tan\theta_0 - |x|)/4, \end{aligned} \tag{10}$$

where $\eta = \chi_{hi}/|\chi_{hr}|$. According to (6) and (10), the intensity distribution (4) on the hologram is

$$\begin{aligned} I_h(p, x, y) = A(p)\Big[& 1 - 2aU^*(p)\,\tilde{S}^*(y)\exp\big(i\Phi_+\big) \\ & - 2aU(p)\,\tilde{S}(y)\exp(i\Phi_-) \\ & + 4a^2\Gamma(p)\,\tilde{S}^*(y)\,\tilde{S}(y)\exp\Big(-\frac{\pi x^2\eta}{T\Lambda_r\tan^2\theta_0}\Big)\Big], \end{aligned} \tag{11}$$

where $\Phi_\pm = \pm\pi x^2(1 \pm i\eta)(2T\Lambda_r\tan^2\theta_0)^{-1} \pm k\cos\theta_0\Delta\theta x$. The notations $A(p) = \exp[-\mu_d(p)T\cos^{-1}\theta_0][4(1 + p^2)]^{-1}$, $U(p) = \Gamma^{1/2}(p)\exp(i\pi/4)\exp[-i\pi Tu(p)\Lambda_r^{-1}]$, $u(p) = (1 + p^2)^{1/2} - 1$, $\delta_d(p) = \mu_d(0) - \mu_d(p)$, $\Gamma(p) = (1 + p^2)\exp[-\delta_d(p)T\cos^{-1}\theta_0]\cot^2\theta_0(2T\Lambda_r)^{-1}$ are also used. The hologram is recorded in the region $|x| < T\tan\theta_0$.

In Fig. 2, using (5) and (7), the numerical calculated intensity distribution (4) for a completely absorbing wire, with the axis perpendicular to the diffraction plane, is shown. The case of Si(220) reflection, $\lambda = 0.71$ Å (17.46 keV) radiation, $\Delta\theta = 0$, $T = 5$ mm, $a = 5$ µm, σ-polarization is taken, $\mu T = 7.3$. In Fig. 3 the hologram of a wire of size $2a = 1$ µm is presented. The contrast is worse since the wire of size $2a = 1$ µm has lower scattering amplitude than the wire of size $2a = 10$ µm. The necessary data are taken from Pinsker (1982).

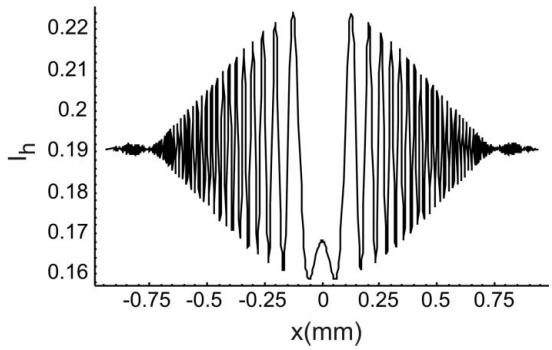

Figure 2
Intensity distribution of a completely absorbing wire on the dynamical diffraction hologram. The size of the wire $2a = 10$ µm.

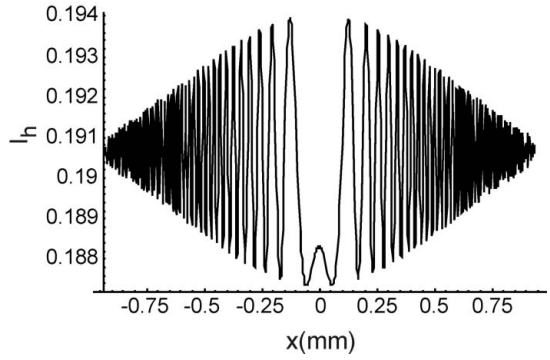

Figure 3
Intensity distribution of a completely absorbing wire on the dynamical diffraction hologram. The size of the wire $2a = 1$ µm.

2.4. X-ray Fraunhofer hologram of an object

If the condition $a \ll |\Lambda|\tan\theta_0/\pi$ is not fulfilled, in (7) one can use the approximation

$$\begin{aligned} \left[T^2\tan^2\theta_0 - (x - x')^2\right]^{1/2} \simeq\ & T\tan\theta_0\big[1 - x^2/(2T^2\tan^2\theta_0) \\ & + xx'/(T^2\tan^2\theta_0) \\ & - x'^2/(2T^2\tan^2\theta_0)\big]. \end{aligned}$$

The quadratic on x' term can be neglected if $\pi a^2/(2T\Lambda_r\tan^2\theta_0) \ll \pi$. This approximation is equivalent to the well known approximation in the Fraunhofer zone of diffraction in visible-light optics. Using this approximation, similarly to (10), one can write

$$\begin{aligned} E_{h\,\mathrm{obj}} \simeq\ & \left(\frac{2}{T\Lambda_r}\right)^{1/2}\exp(i\pi/4)\cot\theta_0\,\tilde{S}(x, y)\exp\left(\frac{i\pi T}{\Lambda_r}\right) \\ & \times \exp\left(\frac{ik\chi_{0r}T}{2\cos\theta_0}\right)\exp\left[-\frac{\mu_d(0)T}{2\cos\theta_0}\right] \\ & \times \exp\left(-\frac{i\pi x^2}{2T\Lambda_r\tan^2\theta_0}\right)\exp\left(-\frac{\pi x^2\eta}{2T\Lambda_r\tan^2\theta_0}\right) \\ & \times H(T\tan\theta_0 - a - |x|)/4, \end{aligned} \tag{12}$$

but now

$$\tilde{S}(x,y) = \int_{-a}^{a} S(x',y)\exp[i\pi xx'/(T\Lambda_r\tan^2\theta_0)] \times \exp(ik\cos\theta_0\Delta\theta x')\,dx',$$

i.e. as in the visible-light optics $\tilde{S}(x,y)$ is the Fourier transform of $S(x,y)$. Inserting (6) and (12) into (4) for the intensity distribution on the hologram we have

$$I_h(p,x,y) = A(p)\Big[1 - U^*(p)\,\tilde{S}^*(x,y)\exp(i\Phi_+) - U(p)\,\tilde{S}(x,y)\exp(i\Phi_-) + \Gamma(p)\,\tilde{S}^*(x,y)\,\tilde{S}(x,y)\exp\Big(-\frac{\pi x^2\eta}{T\Lambda_r\tan^2\theta_0}\Big)\Big]. \quad (13)$$

The hologram is recorded in the region $|x| < T\tan\theta_0 - a$. This formula is equivalent to the Fraunhofer hologram intensity distribution in visible-light optics (Caulfield, 1979).

2.5. Requirements of temporal and spatial coherence of the incident X-ray beam

The formulae above are written for a monochromatic beam and for a source with zero size. Real incident beams are not monochromatic and real sources have finite sizes. The coherence requirements can be obtained by the method described by Mocella *et al.* (2000). The polychromaticity and the source size do not change the intensity profile on the hologram if

$$2T\tan\theta_0\sin\theta_0 \ll \lambda^2/(2\Delta\lambda_m) = l_c, \quad (14)$$

$$2T\sin\theta_0\, l \ll \lambda L_s, \quad (15)$$

where l_c is the longitudinal coherence length, $\lambda_m - \Delta\lambda_m < \lambda < \lambda_m + \Delta\lambda_m$, l is the source size in the diffraction plane and L_s is the mean distance of the source from the crystal.

3. Reconstruction by visible light using an X-ray Fraunhofer hologram

For reconstruction the hologram is placed in the path of visible light. We assume a linear recording range of the hologram recording process. Also the amplitude transmittance of the hologram is a linear function of the intensity registered by the hologram (Hariharan, 2002). The light passing through the hologram and diffracting in a vacuum can give the real and the virtual images of the object. In the visible-light optics at a certain distance from the hologram the second term of (4) gives the real direct image of the object and can be registered without any lens; meanwhile the third term gives the virtual image of the object and reconstructs the field of the object with its amplitudes and phases. This part of the reconstructed field can be registered visually or by using a lens. In the X-ray case, when only the weakly absorbing branch of σ-polarization is taken into account, the real image is formed by the third term of (4). This assumption is clearly seen from (11) and (13).

In this section the coordinates x, y, z are parallel to the corresponding coordinates connected with the crystal, but now z is counted perpendicular to the hologram plane ($z = 0$). We assume that the disturbance incident on the hologram wave is a scalar monochromatic spherical wave with amplitude $\exp[ik_0(x^2+y^2)/(2L_0)]/L_0$, where L_0 is the distance of the source from the hologram. The wave propagates along the Oz axis perpendicular to the hologram plane. According to the Huygens–Fresnel principle the amplitude of the light at a distance $z = L$ is given as a convolution,

$$E_{rec} = \frac{1}{L_0}\int_{-\infty}^{+\infty} P(x-x',y-y',L) \times \exp\Big[ik_0\,\frac{x'^2+y'^2}{2L_0}\Big] I_h(x',y')\,dx'\,dy', \quad (16)$$

where the integration is performed along the plane of the hologram (the constant amplitude of the incident wave is taken as 1) and $P(x,y,z) = -ik_0(2\pi z)^{-1}\exp[ik_0(x^2+y^2)/(2z)]$ is the Fresnel propagator (Paganin, 2006), $k_0 = 2\pi/\lambda_0$ is the wavenumber and λ_0 is the wavelength of visible light.

3.1. Reconstruction by visible light using a point object X-ray hologram

In this case formula (11) can be used. Inserting the first term of (11) into (16) and performing integration one obtains the reconstructed reference wavefield amplitude (propagating along Oz) at a distance $z = L$,

$$E_{rec1} = \frac{A(p)}{(L+L_0)}\exp\Big[ik_0\,\frac{x^2+y^2}{2(L+L_0)}\Big]. \quad (17)$$

Here the subscript 1 means the reconstructed field amplitude of the first term of (11). For the amplitude of the reconstructed field of the third term of (11), one can find

$$E_{rec3} = -2aA(p)U(p)\,\bar{\bar{S}}_3(y,L)\,\frac{\exp\big[ik_0(x^2/2L)\big]}{L_0^{1/2}(1-L/L_f+i\eta L/F)^{1/2}} \times \exp\Big[-ik_0\,\frac{(x+Lk\cos\theta_0\Delta\theta/k_0)^2}{2L(1-L/L_f+i\eta L/F)}\Big], \quad (18)$$

where

$$\bar{\bar{S}}_3(y,L) = \exp(-i\pi/4)\Big(\frac{k_0}{2\pi LL_0}\Big)^{1/2}\int_{-\infty}^{+\infty}\int_{-a}^{a} S(x',y') \times \exp\Big\{ik_0\Big[\frac{(y-y')^2}{2L}+\frac{y'^2}{2L_0}\Big]\Big\}\,dx'\,dy'/(2a), \quad (19)$$

$$F = \frac{2T\tan^2\theta_0\cos\theta_0}{|\chi_{hr}|}\frac{\lambda}{\lambda_0}, \quad (20)$$

$$1/L_0 + 1/L_f = 1/F. \quad (21)$$

If $S(x,y)$ is a slowly varying function of y then integration over y' can be performed by the stationary phase method and finally

$$\bar{\bar{S}}_3(y, L) = \left(\frac{1}{L + L_0}\right)^{1/2} \exp\left[ik_0 \frac{y^2}{2(L + L_0)}\right] \times \int_{-a}^{a} S\left[x', yL_0/(L + L_0)\right] \mathrm{d}x'/(2a). \quad (22)$$

The term (18) corresponds to the real direct image of the object. The real image geometrically is focused at the distance L_f, defined in (21). The x_f coordinate of the focused image on the geometrical focusing plane is defined by the relation

$$x_\mathrm{f} = -(\lambda/\lambda_0) L_\mathrm{f} \cos\theta_0 \Delta\theta. \quad (23)$$

The focus spot size on the geometrical focusing plane is

$$\Delta x_\mathrm{f} = (L_\mathrm{f}/F)(\eta F/k_0)^{1/2}. \quad (24)$$

The minimum size of the focus point is reached at the distance

$$L'_\mathrm{f} = \frac{L_\mathrm{f}}{1 + \eta^2 (L_\mathrm{f}/F)^2}. \quad (25)$$

According to (25) the distance L'_f is approximately equal to L_f when $(L_\mathrm{f}/F)^2 \ll 1/\eta^2$. Since $\eta \simeq 10^{-2}$ then for $L_\mathrm{f} \geq 10^2 F$ the distance L'_f can significantly differ from L_f. The focus spot size at the distance L'_f is defined by the expression

$$\Delta x'_\mathrm{f} = \frac{L_\mathrm{f}}{F\left[1 + \eta^2 (L_\mathrm{f}/F)^2\right]^{1/2}} \left(\frac{\eta F}{k_0}\right)^{1/2}. \quad (26)$$

If any other point object is placed along Ox at the distance Δ_x from the first one, then the focus coordinate of the second object will be

$$x_\mathrm{f1} = -(\lambda/\lambda_0) L_\mathrm{f} \cos\theta_0 \Delta\theta + L_\mathrm{f} \Delta_x / F. \quad (27)$$

Thus the image is direct and the distance between the images is $x_\mathrm{f1} - x_\mathrm{f} = L_\mathrm{f} \Delta_x / F$. The magnification

$$M = (x_\mathrm{f1} - x_\mathrm{f})/\Delta_x = L_\mathrm{f}/F. \quad (28)$$

As can be seen from (18), the centre of the real image propagates along the direction which forms with Oz an angle

$$\psi = -(\lambda/\lambda_0) \cos\theta_0 \Delta\theta. \quad (29)$$

If $\Delta\theta \neq 0$, the real image and the reconstructed reference wave are separated.

Similarly, for the amplitude of the reconstructed field of the second term of (11) we find

$$E_\mathrm{rec2} = -2aA(p)U^*(p)\,\bar{\bar{S}}_2(y, L) \times \frac{\exp\left[ik_0(x^2/2L)\right]}{L_0^{1/2}(1 - L/L_\mathrm{f2} + i\eta L/F)^{1/2}} \times \exp\left[-ik_0 \frac{(x - Lk\cos\theta_0 \Delta\theta/k_0)^2}{2L(1 - L/L_\mathrm{f2} + i\eta L/F)}\right], \quad (30)$$

where

$$1/L_0 + 1/L_\mathrm{f2} = -1/F \quad (31)$$

and

$$\bar{\bar{S}}_2(y, L) = \left(\frac{1}{L + L_0}\right)^{1/2} \exp\left[ik_0 \frac{y^2}{2(L + L_0)}\right] \times \int_{-a}^{a} S^*\left[x', yL_0/(L + L_0)\right] \mathrm{d}x'/(2a). \quad (32)$$

The distance L_f2 is the distance of the reconstructed virtual image of the object and $L_\mathrm{f2} < 0$. The virtual image coordinate is defined as

$$x_\mathrm{f2} = (\lambda/\lambda_0) L_\mathrm{f2} \cos\theta_0 \Delta\theta. \quad (33)$$

According to (33) the reconstructed virtual image centre propagates along the direction which, with Oz, forms an angle $-\psi$. Thus the angle between the directions of propagation of the real and virtual images is $2|\psi|$. This means that, in the case $\Delta\theta \neq 0$, the proposed holographic scheme is an off-axis scheme.

Since the focus spot size (24) and the magnification (28) are proportional to L_f/F, the resolution of the scheme for the hologram with infinite size can be estimated as

$$\Delta_\mathrm{res} \simeq 2(\eta F/k_0)^{1/2}. \quad (34)$$

The reconstructed field amplitude of the fourth term of (11) is proportional to $4a^2$ and is small compared with the first, second and third terms (the second and third terms are proportional to $2a$) of the reconstructed field. This term of the reconstructed field has a Gaussian form and propagates along Oz. The half-width of the Gaussian increases with increasing L and the amplitude decreases. In visible-light optics this term is the so-called autocorrelation of the object image. This term is not considered below.

For the example considered in §2.2 and for $\lambda_0 = 0.65$ µm, using (20) one can estimate $F = 19.8$ mm $\simeq 20$ mm. Since F is sufficiently small, significant magnification can be achieved. The resolution (34) can be estimated, $\Delta_\mathrm{res} \simeq 8$ µm. In Figs. 4 and 5 the numerically calculated intensity distributions $|E_\mathrm{rec}|^2$ [see (16)] in the focusing plane ($z = F$) corresponding to the cases in Figs. 2 and 3 are shown. It is assumed that the image is reconstructed by a monochromatic scalar plane wave. As seen in Figs. 4 and 5, the image of the wire is completely reconstructed. It is interesting to compare Figs. 2, 3 and Figs. 4, 5 with the corresponding results in visible-light optics (Caulfield, 1979). The comparison shows the obvious analogy between the results.

3.2. Reconstruction by visible light using a Fraunhofer X-ray hologram

In this case we must use the formula (13). Instead of the formula (18) now we obtain

$$E_\mathrm{rec3} = -A(p)U(p)\,\bar{\bar{S}}(x, y, L) \times \frac{\exp\left[ik_0(x^2/2L)\right]}{L_0^{1/2}(1 - L/L_\mathrm{f} + i\eta L/F)^{1/2}}, \quad (35)$$

where

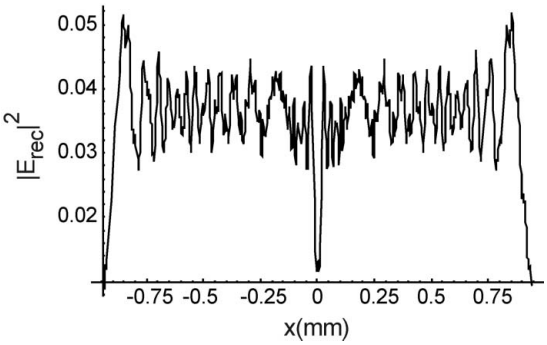

Figure 4
Intensity distribution on the focusing plane of the real image of the wire reconstructed by visible light. The size of the wire $2a$ = 10 µm.

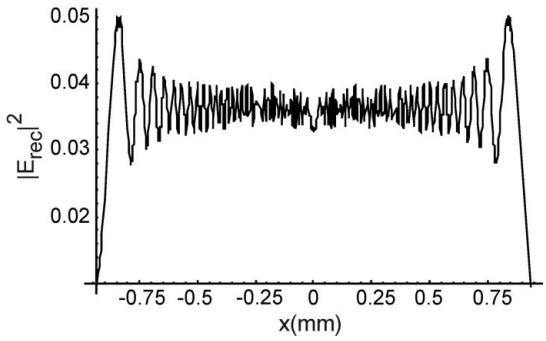

Figure 5
Intensity distribution on the focusing plane of the real image of the wire reconstructed by visible light. The size of the wire $2a$ = 1 µm.

$$\bar{\bar{S}}(x, y, L) = \left(\frac{1}{L+L_0}\right)^{1/2} \exp\left[ik_0\ \frac{y^2}{2(L+L_0)}\right] \times \int_{-a}^{a} S\left[x', yL_0/(L+L_0)\right] \exp(ik\cos\theta_0\Delta\theta x') \times \exp\left[-ik_0\frac{(x+Lk\cos\theta_0\Delta\theta/k_0 - x'L/F)^2}{2L(1-L/L_f+i\eta L/F)}\right] dx'. \quad (36)$$

One can perform the integration over x' taking out under the integral sign the value of $S(x', y')$ at the point $x' = (x + Lk\cos\theta_0\Delta\theta/k_0)F/L$. After performing the integration over x' for E_{rec3}, one finds

$$E_{rec3} = -\left(\frac{2\pi L}{k_0L_0}\right)^{1/2}\frac{F}{L}\ A(p)U(p) \times \exp(-i\pi/4)\exp\left(ik_0\frac{x^2}{2L}\right) S_3(x, y, L), \quad (37)$$

where

$$S_3(x, y, L) = \left(\frac{1}{L+L_0}\right)^{1/2} \exp\left[ik_0\ \frac{y^2}{2(L+L_0)}\right] \times \exp\left[ik\cos\theta_0\Delta\theta\ \frac{F(x+Lk\cos\theta_0\Delta\theta/k_0)}{L}\right] \times \exp\left[ik_0\ \frac{(1-L/L_f)(kF\cos\theta_0\Delta\theta/k_0)^2}{2L}\right] \times \exp\left[-\frac{(\Delta_{res}k\cos\theta_0\Delta\theta)^2}{2}\right] \times S[F(x+Lk\cos\theta_0\Delta\theta/k_0)/L, yL_0/(L+L_0)]. \quad (38)$$

The expressions (37) and (38) are valid near the real image distances $L \simeq L_f$. The centre of the real image propagates along the line $x = -Lk\cos\theta_0\Delta\theta/k_0 = L\psi$. In the same way,

$$E_{rec2} = -\left(\frac{2\pi L}{k_0L_0}\right)^{1/2}\frac{F}{L}\ A(p)U^*(p)\exp(-i\pi/4) \times \exp\left(ik_0\ \frac{x^2}{2L}\right) S_2(x, y, L), \quad (39)$$

where

$$S_2(x, y, L) = \left(\frac{1}{L+L_0}\right)^{1/2} \exp\left[ik_0\ \frac{y^2}{2(L+L_0)}\right] \times \exp\left[ik\cos\theta_0\Delta\theta\ \frac{F(x-Lk\cos\theta_0\Delta\theta/k_0)}{L}\right] \times \exp\left[ik_0\ \frac{(1-L/L_{f2})(kF\cos\theta_0\Delta\theta/k_0)^2}{2L}\right] \times \exp\left[-\frac{(\Delta_{res}k\cos\theta_0\Delta\theta)^2}{2}\right] \times S^*[-F(x-Lk\cos\theta_0\Delta\theta/k_0)/L, yL_0/(L+L_0)]. \quad (40)$$

The centre of the virtual image propagates along the line $x = Lk\cos\theta_0\Delta\theta/k_0 = -L\psi$. The scheme is an off-axis holographic scheme, since the real and virtual images are separated when $\Delta\theta \neq 0$. The formulae (39) and (40) are valid near the distances of the virtual image distance L_{f2}. For any distance L the field (39) propagates according to the Huygens–Fresnel principle (16).

4. Conclusions

In this paper an X-ray dynamical diffraction Fraunhofer holography scheme is proposed and theoretically investigated. An object is placed in the path of a plane X-ray beam incident on the entrance surface of a crystal. In the Laue symmetrical two-wave diffraction case on the exit surface of the crystal the interference pattern of the reference plane wave and the object wave is formed. By recording this interference pattern in the diffracted field the hologram of the object is obtained. Two cases are discussed: the case of a point object and Fraunhofer hologram recording. The coherence requirements of the incident beam are discussed. The illumination of the hologram by visible light reconstructs the real and the virtual images of the object. Expressions of the focusing distance of the real and virtual images as well as of magnification are obtained. It is shown that in the case $\Delta\theta \neq 0$ the proposed scheme is an off-axis holographic scheme. Expressions of the focus spot size and resolution are presented. Since the focal distance is sufficiently small, significant magnification can be obtained. As an example, X-ray hologram recording and

visible-light reconstruction for an absolutely absorbing wire are considered theoretically. Numerical calculations show that the object real image on the focusing plane is completely reconstructed. The obtained results are compared with the corresponding results in visible-light optics. The comparison shows the obvious analogy between the results.

The reconstruction can be performed also using numerical (mathematical) methods of reconstruction. The proposed scheme can be used in X-ray microscopy. Experimental realisation can be performed using synchrotron X-ray sources.

It would be interesting to investigate the influence of the asymmetry factor on the properties of the discussed scheme, *i.e.* on the resolution, on the hologram size, on the coherence requirements, *etc.* Another development of the X-ray dynamical diffraction holographic scheme can be a Fourier holographic scheme based on double-slit dynamical diffraction (Balyan, 2010). In this case an object and a narrow slit must be placed in front of a crystal in the way of a collimated incident X-ray beam. The recorded interference pattern of an object wave and the wave emerged from the slit can be regarded as an X-ray Fourier hologram of the object. The subsequent reconstruction must be performed by visible-light or by numerical (mathematical) methods of reconstruction.

The author is grateful to Dr K. T. Gabrielyan for useful discussions which have stimulated this work.

References

Anduleit, K. & Materlik, G. (2003). *Acta Cryst.* A**59**, 138–142.
Aristov, V. V. & Ivanova, G. A. (1979). *J. Appl. Cryst.* **12**, 19–24.
Authier, A. (2001). *Dynamical Theory of X-ray Diffraction.* Oxford University Press.
Balyan, M. K. (2010). *Acta Cryst.* A**66**, 660–668.
Caulfield, H. J. (1979). Editor. *Handbook of Optical Holography.* New York: Academic Press.
Chukhovskii, F. N. & Poliakov, A. M. (2004). *Acta Cryst.* A**60**, 82–88.
Egiazaryan, A. M., Trouni, K. G. & Mkrtchyan, A. R. (1998). *Pisma Zh. Exp. Teor. Fiz.* **68**, 681–684.
Egiazaryan, A. M. (1998). *Pisma Zh. Tech. Fiz.* **24**, 55–59.
Egiazaryan, A. M. & Bezirganyan, P. A. (1980). *Proc. Nat. Acad. Sci. Armen. Phys.* **15**, 35–43.
Gabrielyan, K. T. (1990). *Pisma Zh. Tech. Fiz.* **16**, 5–9.
Hariharan, P. (2002). *Basics of Holography.* Cambridge University Press.
Hau-Riege, S. P., Szoke, H., Chapman, H. N., Szoke, A., Marchesini, S., Noy, A., He, H., Howells, M., Weierstall, U. & Spence, J. C. H. (2004). *Acta Cryst.* A**60**, 294–305.
Iwamoto, H. & Yagi, N. (2011). *J. Synchrotron Rad.* **18**, 564–568.
Kopecký, M. (2004). *J. Appl. Cryst.* **37**, 711–715.
Korecki, P., Novikov, D. V., Tolkiehn, M. & Materlik, G. (2004). *Phys. Rev. B*, **69**, 184103.
Leitenberger, W. & Snigirev, A. (2001). *J. Appl. Phys.* **90**, 538.
Mocella, V., Epelboin, Y. & Guigay, J. P. (2000). *Acta Cryst.* A**56**, 308–316.
Momose, A. (1995). *Nucl. Instrum. Methods Phys. Res. A*, **352**, 622–628.
Novikov, D. V., Adams, B., Hiort, T., Kossel, E., Materlik, G., Menk, R. & Walenta, A. (1998). *J. Synchrotron Rad.* **5**, 315–319.
Nugent, K. A., Gureyev, T. E., Cookson, D. J., Paganin, D. & Barnea, Z. (1996). *Phys. Rev. Lett.* **77**, 2961–2964.
Nygård, K., Bunk, O., Perret, E., David, C. & van der Veen, J. F. (2010). *J. Appl. Cryst.* **43**, 350–351.
Paganin, D. M. (2006). *Coherent X-ray Optics.* Oxford University Press.
Pinsker, Z. G. (1982). *X-ray Crystallooptics.* Moscow: Nauka. (In Russian.)
Slobodetskii, I. Sh. & Chukhovskii, F. N. (1970). *Kristallografiya*, **15**, 1101–1107.
Snigirev, A., Snigireva, I., Kohn, V., Kuznetsov, S. & Schelokov, I. (1995). *Rev. Sci. Instrum.* **68**, 5486–5492.
Szöke, A. (1998). *Acta Cryst.* A**54**, 543–562.
Watanabe, N., Yokosuka, H., Ohogashi, T., Takano, H., Takeuchi, A., Suzuki, Y. & Aoki, S. (2003). *J. Phys. IV Fr.* **104**, 551–556.